17th Brazilian Congress of Thermal Sciences and Engineering
November 25th-28th, 2018, Águas de Lindóia, SP, Brazil

ENCIT-2018-0789
AERODYNAMIC ANALYSIS OF A SCRAMJET FOR ATMOSPHERIC FLIGHT

Paulo Gilberto de Paula Toro
Elder Samuel Taveira da Silva
Jonatha Wallace Silva de Araújo
George Santos Marinho
Universidade Federal do Rio Grande do Norte / UFRN - Centro de Tecnologia – Departamento de Engenharia Mecânica.
Av. Senador Salgado Filho, 3000 - Campus Universitário, Lagoa Nova CEP 59.078-970 – Natal / RN - Brasil
toro@ct.ufrn.br; elder-samuelts @hotmail.com, jonatha_wallace@hotmail.com; gmarinho@ct.ufrn.br

Gilvan Luiz Borba
Universidade Federal do Rio Grande do Norte / UFRN - Centro de Ciencias Exatas e da Terra – Departamento de Geofísica.
Av. Senador Salgado Filho, 3000 - Campus Universitário, Lagoa Nova, CEP 59.078-970 – Natal / RN - Brasil
gilvan@geofisica.ufrn.br

Israel da Silveira Rêgo
Instituto de Estudos Avançados / IEAv - Trevo Coronel Aviador José Alberto Albano do Amarante, nº1 Putim CEP. 12.228-001
São José dos Campos, SP - Brasil
israel.rego@ieav.ct.br

Abstract. *This paper presents an aerodynamic conception of an academic scramjet designed for a flight at 6.2 km of altitude with a speed corresponding to Mach number 4.18, which will be coupled to the intermediate training rocket (FTI) of the Barreira do Inferno Launch Center (CLBI) in Rio Grande do Norte (RN), Brazil. The current means of access to space is limited by the quantity of fuel that rockets need to take to get out of the dense layers of the atmosphere, which causes little payload to be boarded, limiting aerospace activities. The scramjet technological demonstrator is being studied as a new technology of access to space, as this technology proposes a new system of airbreathing propulsion. The proposed academic scramjet will be coupled in the FTI, functioning as a second stage in order to obtain more power during the flight. Calculations were made in the geometry variation in order to select the best compression and expansion section for the scramjet, with heat addition. In the compression section, only one configuration with three tamps was considered. The analytical results were compared with simulation results.*

Keywords: *scramjet, hypersonics, shock waves, thermal properties, numerical simulation.*

1. INTRODUCTION

New technologies are being developed to facilitate man's move to space, much of it to improve rocket power. Currently, about 80% of the weight of the rockets consists only of fuel for their propulsion and the remaining 20% is their structure and payload. This large amount of fuel makes it difficult to develop technologies and bring more payload to space (satellites, research development and others). The need to develop technology to reduce the weight of the rocket to bring more payload to the space, the aerospace vehicles that use airbreathing propulsion system based on supersonic combustion (scramjet). Its operating principle is based on the convenient use of the oblique / conical shockwaves generated in the compression section (front of the vehicle) during hypersonic flight to compress and decelerate atmospheric air to supersonic speeds at the combustion chamber inlet, reaching thus the properties required for the spontaneous combustion of the injected fuel. In Brazil the Instituto de Estudos Avançados (IEAv) develops the scramjet 14-X waverider (Fig. 1).

The IEAv also develops other scramjet models, evaluating their performance. The 14-X B (Fig. 2) is being designed at the Laboratório de Aerotermodinâmica e Hipersônica Prof. Henry T. Nagamatsu, at the Instituto de estudos avançados (IEAv) since March 2012, as an option to demonstrate the hypersonic airbreathing propulsion system based on supersonic combustion at free flight at 30km altitude at Mach number 7, using Brazilian two-stage rocket engines (S31 and S30), which are able to boost the 14-X B to the predetermined conditions of the scramjet operation, 30km altitude at Mach number 7 (Galvão and Toro, 2013)

Figure 1. Brazilian Technological scramjet 14-X waverider.

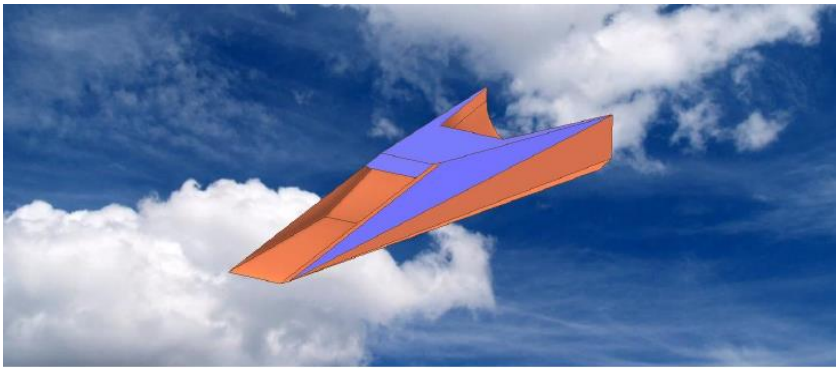

Figure 2. Hypersonic Aerospace Vehicle 14-X B.

As an objective to promote the airbreathing hypersonic propulsion. Now, the academic scramjet appears with an opportunity to train the students and spread the knowledge in airbreathing propulsion systems of in Brazilian universities, as it is being developed in the Universidade Federal do Rio Grande do Norte (UFRN).

2. METHODOLOGY

The terminology of this work is the same nomenclature presented by Heiser and Pratt (1994), which defines the compression sections (external and internal), combustion section and expansion section (internal and external) of a scramjet. This definition makes it possible to analyze the thermodynamic cycle in the engine and, consequently, to determine the efficiency of the propulsion system, figure 3.

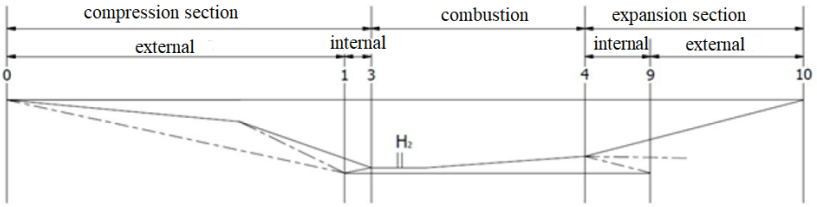

Figure 3. The terminology of scramjet.

The calculations were made in the geometry variation in order to select the best compression and expansion section for the scramjet. In the compression section, one configuration with three ramps was considered, the first one has 6º, a second ramp with 6.7º and the third ramp with 7.52°. Also, was considered heat addition in combustion chamber.

2.1 INCIDENT OBLIQUE SHOCK WAVE

The incident oblique shock wave is established on the leading edge of a wedge-shaped body at supersonic or hypersonic velocities. The establishment of this wave compresses the air of the atmosphere between the surface of the body and the shock wave. The result of this compression is the increase of thermodynamic properties as pressure, temperature, specific mass and speed sound, also the decrease as flow velocity and Mach number (Fig. 4).

From the relations of the oblique shock wave, (Eq. (1) to (4) presented by Anderson (2003)) it is possible determine the properties of the flow after the shock, considering the air with perfect gas behavior and not viscous flow. The relation θ - β - M, is given by Eq. (5), allows to obtain known θ and M.

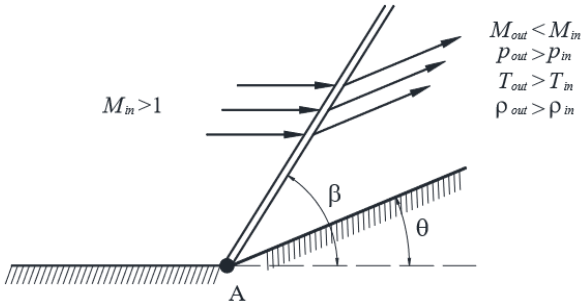

Figure 4. Incident oblique shock wave.

$$\frac{p_{out}}{p_{in}} = 1 + \frac{2\gamma}{(\gamma+1)}\left[(M_{in} sen\beta)^2 - 1\right] \tag{1}$$

$$\frac{\rho_{out}}{\rho_{in}} = \left[\frac{(\gamma+1)(M_{in} sen\beta)^2}{(\gamma-1)(M_{in} sen\beta)^2 + 2}\right] \tag{2}$$

$$\frac{T_{out}}{T_{in}} = \frac{p_{out}}{p_{in}} \cdot \frac{\rho_{in}}{\rho_{out}} \tag{3}$$

$$M_{out} = \frac{\sqrt{\dfrac{(M_{in} sen\beta)^2 + \dfrac{2}{(\gamma-1)}}{\dfrac{2\gamma}{(\gamma-1)}(M_{in} sen\beta)^2 - 1}}}{sen(\beta-\theta)} \tag{4}$$

$$tg\theta = 2\,\mathrm{cotg}\,\beta\left[\frac{(M_{in} sen\beta)^2 - 1}{M_{in}^2(\gamma + \cos 2\beta) + 2}\right] \tag{5}$$

2.2 REFLECTED OBLIQUE SHOCK WAVE

After the incident oblique shock wave has been established, if the deflected flow encounters a flat surface, it will cause reflection of the incident wave, called the reflected oblique shock wave (Fig. 5). The flow of this shock wave must adjust to the contour conditions, being parallel to the surface. The same relations use to the incident oblique shock wave may be use to reflected oblique shock wave (Anderson, 2003).

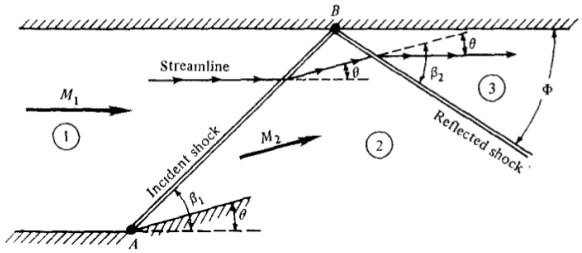

Figure 5. Reflected oblique shock wave.

2.3 EXPANSION WAVE

When the supersonic or hypersonic flow on a flat plate encounters a negative deflection, this flow needs to adjust to the new direction, then the expansion wave (Fig 6) is established. The adjustment of the flow will occur in such a way that its original direction will be altered by a wave of continuous expansion, as a result, there will be an increase in the flow velocity and Mach number, and a decrease in pressure, temperature and specific mass (Anderson, 2003). The Eq. (6), (7) and (8), represent, respectively, the ratio of temperature, the pressure ratio and the specific mass ratio through the expansion range.

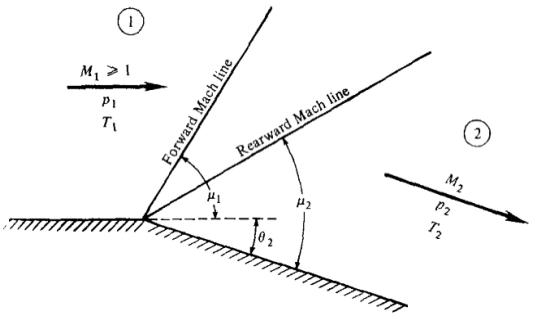

Figure 6. Expansion wave.

$$\frac{T_{out}}{T_{in}} = \frac{1+\frac{\gamma-1}{2}M_{in}^2}{1+\frac{\gamma-1}{2}M_{out}^2} \tag{6}$$

$$\frac{p_{out}}{p_{in}} = \left[\frac{1+\frac{\gamma-1}{2}M_{in}^2}{1+\frac{\gamma-1}{2}M_{out}^2}\right]^{\frac{\gamma}{\gamma-1}} \tag{7}$$

$$\frac{\rho_{out}}{\rho_{in}} = \left[\frac{1+\frac{\gamma-1}{2}M_{in}^2}{1+\frac{\gamma-1}{2}M_{out}^2}\right]^{\frac{1}{\gamma-1}} \tag{8}$$

In the expansion wave theory, the Prandtl-Meyer function, is given by Eq.(9).

$$\upsilon(M) = \sqrt{\frac{\gamma+1}{\gamma-1}}tg^{-1}\sqrt{\frac{\gamma-1}{\gamma+1}(M^2-1)} - tg^{-1}\sqrt{M^2-1} \tag{9}$$

The angle of deflection of the flow θ, is obtained by the function of Prandtl-Meyer υ before and after the expansion fan, is given by Equation (10)

$$\theta = \upsilon(M_{out}) - \upsilon(M_{in}) \tag{10}$$

2.4 HEAT ADDITION IN COMBUISTION CHAMBER

Operation of a scramjet may involve the injection of fuel into the combustion chamber, where the chosen fuel is mixed into the atmospheric air at supersonic speed, causing combustion if the temperature conditions are adequate Operation of a scramjet may involve the injection of fuel into the combustion chamber, where the chosen fuel is mixed into the atmospheric air at supersonic speed, causing combustion if the temperature conditions are adequate.

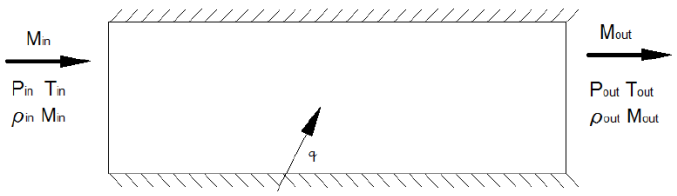

Figure 7. One-dimensional with constant-area heat addition.

Mass, momentum and energy conservation laws (Anderson, 2013) can be applied to the one-dimensional with constant area heat addition, and they are given by:

$$\rho_{in} u_{in} = \rho_{out} u_{out} \tag{11}$$

$$p_{in} + \rho_{in} u_{in}^{\,2} = p_{out} + \rho_{out} u_{out}^{\,2} \tag{12}$$

$$h_{in} + \frac{u_{in}^{\,2}}{2} + q = h_{out} + \frac{u_{out}^{2}}{2} \tag{13}$$

The energy equation (Eq. 13) indicates the heat addition change the total energy. For calorically and thermally perfect gas and applying the total temperature definition, obtains

$$q = c_p (\mathrm{T}_{0,out} - T_{0,in})$$

where,

$$\frac{T_0}{T} = 1 + \frac{\gamma - 1}{2} M^2$$

Eq. (14), (15) and (16), represent, respectively, the ratio of temperature, the pressure ratio and the specific mass ratio caused by heat addition.

$$\frac{p_{out}}{p_{in}} = \frac{1 + \gamma M_{in}^2}{1 + \gamma M_{out}^2} \tag{14}$$

$$\frac{T_{out}}{T_{in}} = \left[\frac{1 + \gamma M_{in}^2}{1 + \gamma M_{out}^2} \right]^2 \left[\frac{M_{out}}{M_{in}} \right]^2 \tag{15}$$

$$\frac{\rho_{out}}{\rho_{in}} = \left[\frac{1 + \gamma M_{out}^2}{1 + \gamma M_{in}^2} \right] \left[\frac{M_{in}}{M_{out}} \right]^2 \tag{16}$$

2.5 NUMERICAL HYPERSONIC FLOW ANALYSIS APPLIED TO SCRAMJET

The commercial software Fluent is able to solve the Navier-Stokes equations (continuity, momentum and conservation of energy), considering single-phase and multiphase flow, Newtonian and non-Newtonian fluid, from subsonic to hypersonic velocity, being such software used in numerical simulation of the 14-X Technological Demonstrator.

Some considerations were made for this simulation:

I) The geometry was created in Solidworks software and implemented in ANSYS software (figure 5).
II) Fluid is invisible;
III) There is no addition of heat in the combustion chamber;
IV) Perfect gas;
V) Escoamente in permanent and compressible regime
VI) Adiabatic and two-dimensional;
VII) Vehicle flying at Mach 4,18 to an altitude of 6.2125 km, so the sound speed, static temperature and static density and static pressure, are the same as in table 1.

Knowing the altitude of scramjet operation is 6.2125 km, it can obtain the thermodynamic properties of the air at this altitude, these properties can be obtained by the data of the American standard atmosphere US Standard Atmosphere (1976), the values are shown in the following table 1:

Table 1. Atmospheric properties to 6.2125 km.

Altitude [km]	Temperature [K]	Pressure [kPa]	Specific Mass [kg/m³]	Speed of sound [m/s]
6.2125	247.8	45.86	0.6447	315.6

3. RESULTS

The thermodynamic property ratios and the flow velocity for scramjet design are presented in the following table 2.

Table 2. thermodynamic property ratios along the scramjet.

Properties	Compression ramps			Combustion Chamber Inlet
	1st Ramp	2nd Ramp	3rd Ramp	
M_{in}	4.18	3.7195	3.2843	2.8692
θ_{in} [°]	6	6.7	7.52	20.22
β_{out} [°]	18.1706	20.5137	23.3815	39.1166
M_{out}	3.7196	3.2843	2.8692	1.8964
T_{out}/T_{in}	1.1930	1.1930	1.1930	1.5392
p_{out}/p_{in}	1.8156	1.8154	1.8153	3.6563
ρ_{out}/ρ_{in}	1.5218	1.5217	1.5216	2.3754

Using the above property ratios and the conditions at the Earth's atmosphere, note that now know the properties of each section of the scramjet, the following table 3 shows the results. In order, the last column shows the results with heat addition inside the combustion chamber.

Table 3. Properties of scramjet.

Properties	Inlet	Ramp 6°	Ramp 6.7°	Ramp 7.52°	Combustion Chamber Inlet	Combustion Chamber Outlet
M	4.18	3.7195	3.2843	2.869	1.89	1.2
P[kPa]	45.86	83.263	151.156	274.394	1003.27	1996.203
ρ[kg/m³]	0.6447	0.981	1.493	2.2716	5.396	6.728
T [K]	247.8	295.6254	352.681	420.748	647.62	1033.552
a [m/s²]	315.6	344.648	376.440	411.165	510.110	644.423
u [m/s]	1319.208	1281.918	1236.343	1179.715	964.108	773.307
T_0	1113.732	1113.602	1113.529	1113.495	1110.286	1331.215

Using the ANSYS software, a mesh was generated to simulate the flowfield over the scramjet, this mesh has 217876 nodes and 214618 elements. The results of the simulation that will be shown are temperature, pressure, Mach number and density. The figure 8 shows the mesh developed.

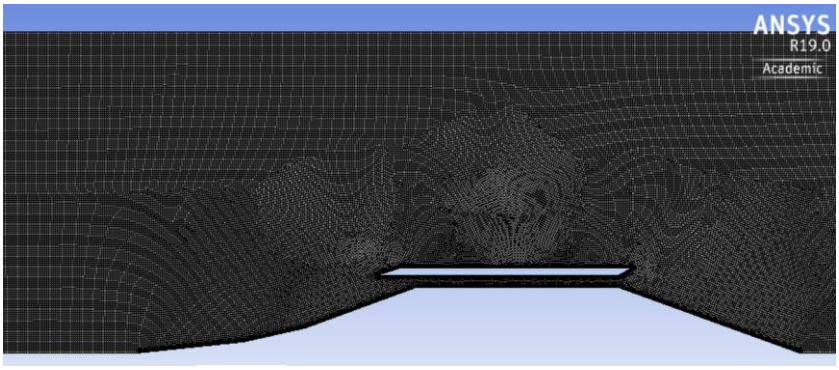

Figure 8. The mesh created to simulation.

After the generation of the mesh, there was a refinement of the edges to improve the simulation, figure 9 shows the refinement around the scramjet, note that the cells are smaller, being 1mm in length.

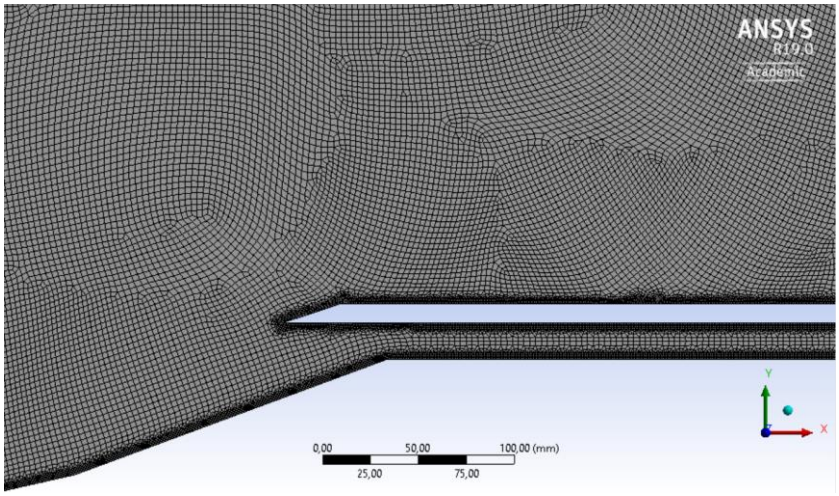

Figure 9. The refinement of mesh.

After the fluent simulation, note that the incident shock waves collide (not too close) at the end of the internal compression section, the same happens with the reflected shock wave at the combustion chamber inlet, which means that all airflow is entering into the combustion chamber, the figure 10 shows the Mach number along the vehicle. Note that, in figure 8, it shows more details inside the combustion chamber, which has the same Mach number as shown in table 3.

In addition, the simulation does not show the variation of properties with addition heat, note that the properties do not change inside the combustion chamber.

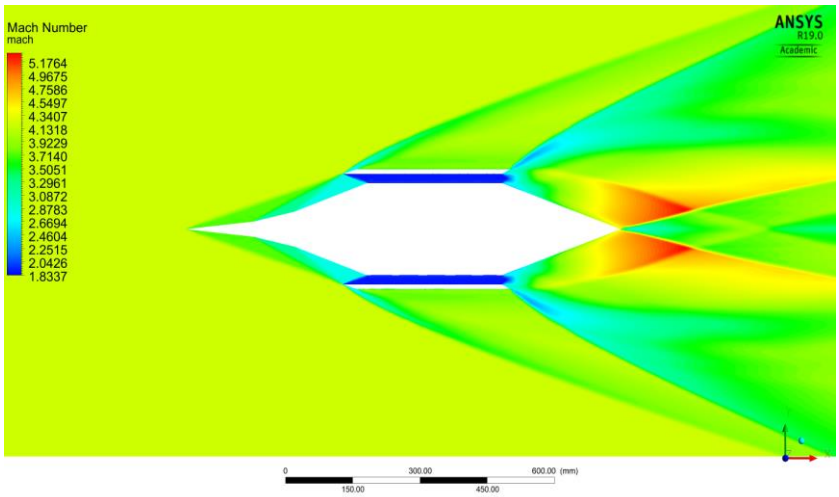

Figure 10. Mach number along the scramjet.

It is also possible to observe the shock waves incident on the ramps of 6°, 6.7° and 7.52°, which provides the decrease of the Mach number, the same can be observed in the reflected shock wave.

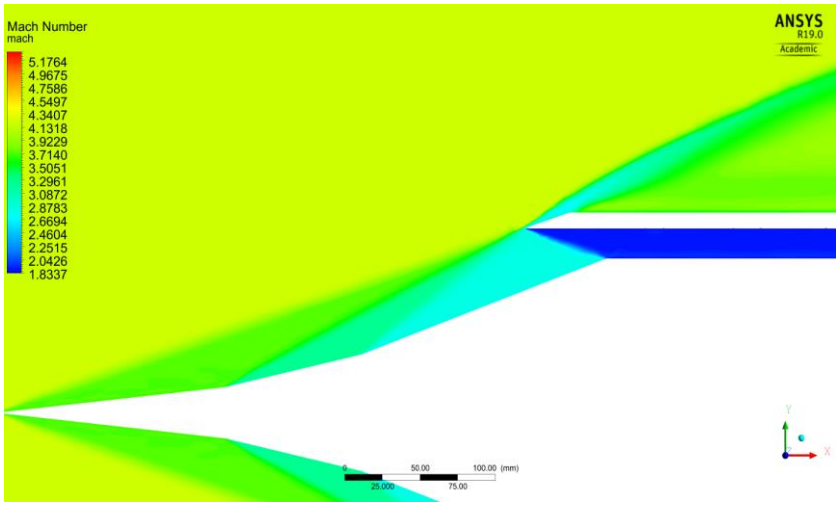

Figure 11. Mach number inside the combustion chamber.

The three compression ramps of the scramjet technological demonstrator are able to generate airflow in the combustion chamber with supersonic Mach number of 1.2 <M <5. (Anderson, 2003) (Fig. 11).

The temperature obtained in the simulation also is close with the theoretical-analytical result, shown in table 3, in the figure 12, the temperature property is shown throughout sections of the vehicle.

Observing the combustion chamber of the scramjet in figures 12 and 13, note that there is a subtle shock train, this is because the incident and oblique shock waves do not coincide with the points of the leading edge of the fairing and the entrance of the combustion chamber, this causes an oscillation in thermodynamic properties.

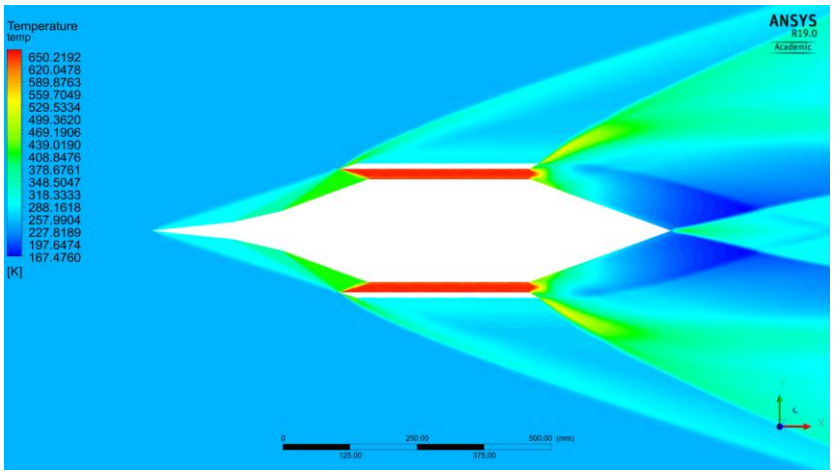

Figure 12. The static temperature along the scramjet.

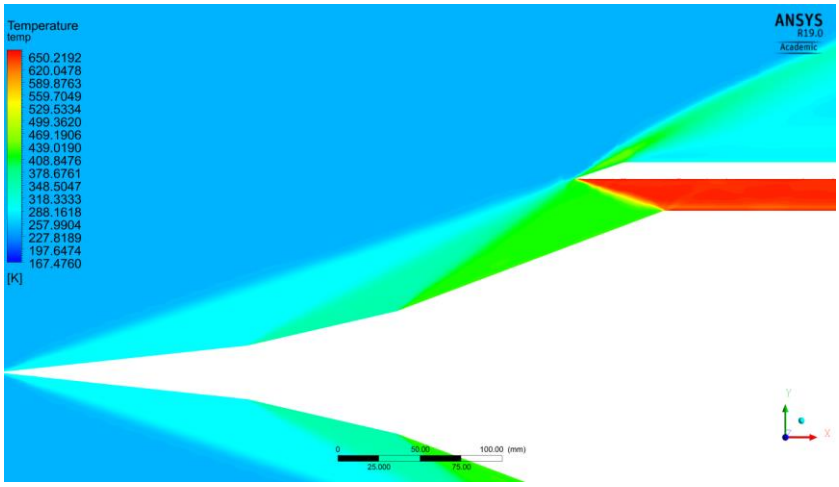

Figure 13. The static temperature inside the combustion chamber.

From the oblique shock wave theory, it can be seen in figure 14 and 15, or increase of the static pressure along the compression ramps, obtaining values close to those found in table 3. Also, it is possible to see a subtle shock train inside of the combustion chamber.

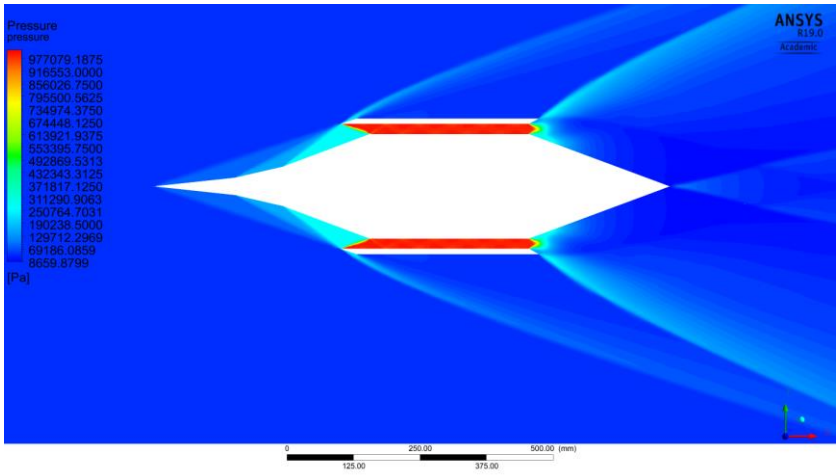

Figure 14. The static pressure along the scramjet.

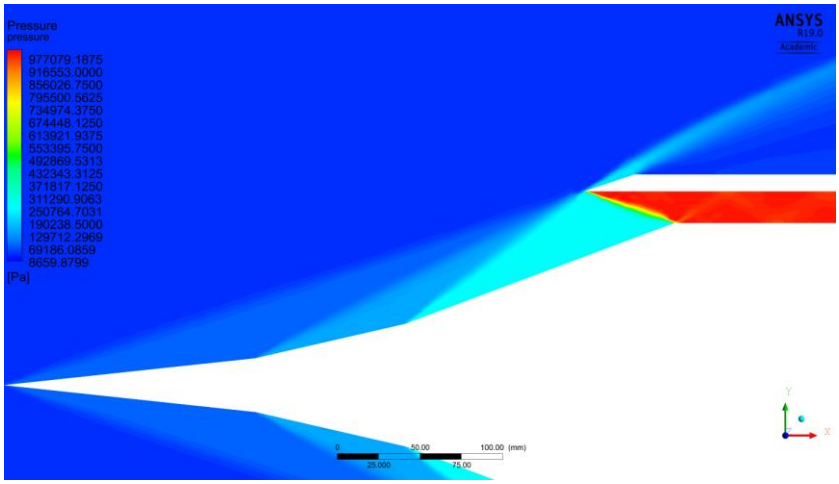

Figure 15. The static pressure inside the combustion chamber.

It is observed that the static density along the compression region increases, as well as the other thermodynamic properties, such as static temperature and static pressure, and after the expansion region the density value decreases as well as the static temperature and static pressure.

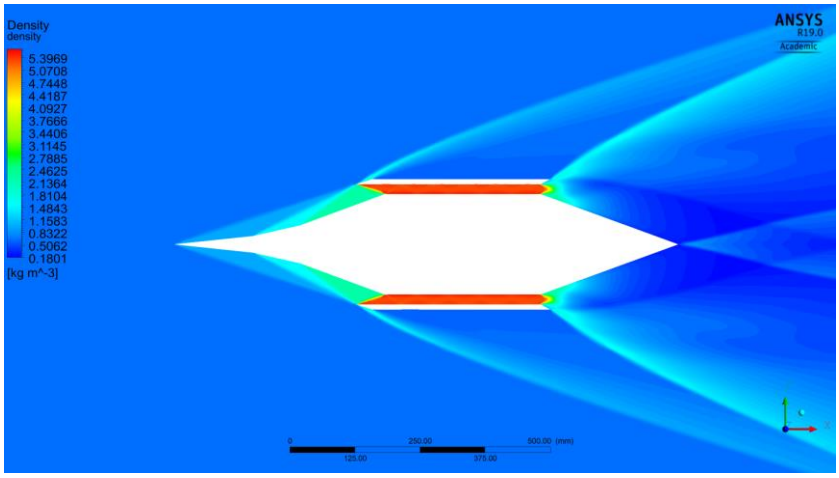

Figure 16. The static density aling the vehicle.

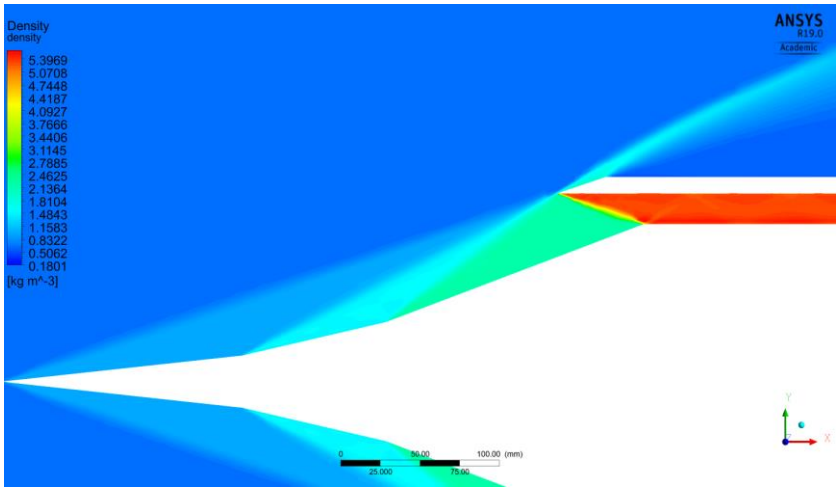

Figure 17. The static density inside the combustion chamber.

4. CONCLUSION

The primary objective of this work is to present a methodology do design a hypersonic vehicle. The incident, reflected, and expansion oblique shock wave theories were used for a theoretical-analytical analysis and to evaluate the aerothermodynamic properties of the flow along the planar symmetry scramjet, which will fly coupled to the FTI. The same properties were obtained through numerical theoretical simulation, made by ANSYS software.

In numerical theoretical simulation, it is possible to observe the change of properties in each section of the vehicle, which provides more details of the results, highlighting the refinement in the contours of the vehicle, but it is not possible to observe the addition of heat through the software used, then the properties remain the same inside the combustion chamber. The results are close with the theoretical analysis, this allows and more analyzes and conclusions can be made using software, validating the operation of the vehicle under study.

The design of academic scramjet also has the purpose of enabling brazilian students to study and develop hypersonic technology, making this technology more accessible in Brazil to involve the research, development and innovation (RD&I), focused in hypersonic area.

5. ACKNOWLEDGEMENTS

The first five authors would like to thanks to Universidade Federal do Rio Grande do Norte (UFRN) the support given to complete this scientific work. The first author (as Visiting Professor) would like to express appreciation to UFRN the possibility to apply the knowledge in aerothermodynamics and hypersonics in the research area in hypersonic airbreathing propulsion based on supersonic combustion ramjet (scramjet) technology. A portion of this effort was supported by Instituto de Estudos Avançados (IEAv) and by the Propulsão Hipersônica 14-X (PropHiper) Project and the last author would like express his appreciation.

6 REFERENCES

ANDERSON, J. D. Modern Compressible Flow, with Historical Perspective. New York: McGraw-Hill, 2003. 760 p. ISBN: 0072424435.

HEISER, W. H.; PRATT, D. T. 1994. Hypersonic Air Breathing Propulsion. [ed.] American Institute of Aeronautics and Astronautics. 1994. Washington D.C : AIAA Education Series., 1994.

U.S. Standard Atmosphere. 1976.NASA TM-X 74335.National Oceanic and Atmospheric Administration. National Aeronautics and Space Administration and United States Air Force.

7 RESPONSIBILITY NOTICE

The authors are the only responsible for the printed material included in this scientific article.

The authors declare that there is no conflict of interest regarding the publication of this scientific article.